Directivity improvement of microstrip antenna by inverse refraction metamaterial

Bilal Tütüncü*, Hamid Torpi* and S. Taha İmeci**

*Department of Electronics and Communications Engineering, Faculty of Electrical & Electronics Engineering, Yildiz Technical University, Istanbul, Turkey
**Department of Electrical and Electronics Engineering, Faculty of Engineering and Natural Sciences, International University of Sarajevo, Bosnia and Herzegovina
*Corresponding Author: bilal1334@gmail.com

ABSTRACT

Due to the properties of inverse refraction, the metamaterials can focus the incident wave and can be used as a lens for high directive antennas. For this purpose, in this study, initially, a metamaterial unit cell is designed to exhibit metamaterial feature at 12 GHz and converted into a periodic layer. The reference antenna and the proposed metamaterial layers are simulated and fabricated. It is observed that the directivity of the reference antenna is increased by 2.74 dB with one layer of the proposed metalayer according to the measurement results. Finally, a double lens layer is used and an increase of 4.08 dB is observed. In the literature, the dimensions of metalayers, that is, used to achieve directivity enhancement, are larger than the patch size, but in this study we achieve a significant improvement with metalayers that have almost the same dimensions as the patch. However, the proposed antenna system is more effective than Ku-band antennas in the literature due to its high directivity compared to similar ones.

Keywords: Metamaterial; microstrip patch antenna; LHM; antenna directivity.

INTRODUCTION

In electromagnetic waves, the direction of energy flow is given by right-hand rule (RHM), but when $\epsilon < 0$ and $\mu < 0$, the medium is Left-Handed and these materials are called Left-Handed Medium (LHM) or metamaterials (MM) (Vesalago, 1968). MMs have been used for many different purposes in different frequency ranges owing these extraordinary properties. These materials have many different potential application areas such as invisibility cloak, high sensitivity sensors, signal absorption, anti-radar devices, and super lenses (Werner *et al*., 2015). Microstrip antenna performance optimization is among these applications at microwave range (Cao *et al.,* 2019; Su and Chen, 2018). Controlling directive emissions of incident waves can be a solution to the low directivity problems of patch antennas and therefore inverse refraction metamaterials could be a remedy. If both the permeability (μ) and the permittivity (ϵ) parameters are set negative at the same frequency, an incident electromagnetic wave is inversely refracted and inverse refraction causes focusing as reported by Vesalago (1968) and as shown in Figure 1.
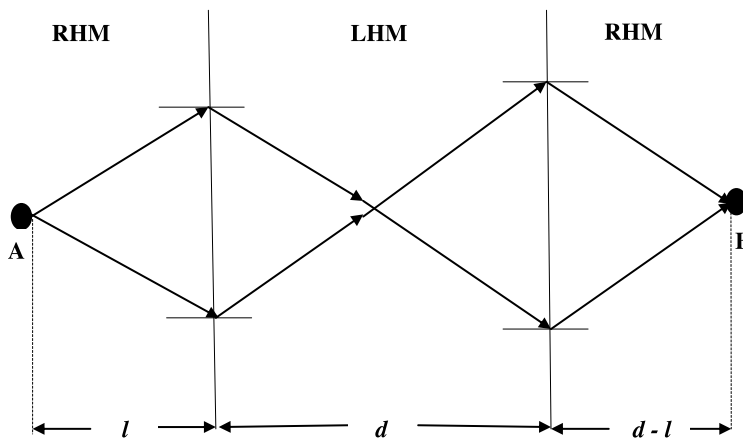
Figure 1. Focusing by inverse refraction.

If the incident wave can be manipulated in the direction of radiation instead of omnidirectional propagation, the directivity and hence the gain will be increased (Pendry, 2000).

In this paper, to confirm this theory, an omega shaped metamaterial (OSM) lens layer is designed and produced for a Ku band reference patch antenna. First of all, a rectangular microstrip patch antenna (MPA) is modeled as reference antenna and with a few experiments in CST, the operating frequency is adjusted around 12 GHz. Fabrication and laboratory measurements are performed at RF and Microwave laboratory. In order to see the increase in directivity by utilizing proposed metalayer, simulation and measurement results of the reference MPA are initially obtained without using OSM layer. Then, an OSM single layer consisting of 2x2 OSM unit cell is placed at a distance of half wavelength of the MPA as a flat lens and results are obtained. A 2.74 dB increase in directivity is observed. Finally, two layers are used, and in this case the increase in directivity is 4.08 dB.

The directivity gain and the size of an antenna are generally mutually conflicting properties. The utilized method in this study has suggested in the literature in recent years, but because of its novelty, it has some deficiencies such as increasing the antenna profile while enhancing the gain (Ma *et al*., 2016; Dhouibi *et al*., 2013; Xu *et al.,* 2014). Increasing superstrate size leads to an inevitable enlargement of overall size and structural complexity of the antenna and surrounding the radiating element by MM structure on a same plate, which causes problems in integrating the radiating element with other components of the goal system (Brito *et al.,* 2012; Mousavi *et al.,* 2013).

Moreover, this improvement has been tried by using different dielectric substrate materials for reference antenna and MM layer with different characteristics (Li *et al.,* 2012; Adel *et al*., 2016). Gain improvement was achieved by a MM unit cell on a dielectric substrate, which has a higher dielectric constant than the substrate of the reference antenna, whereas it is known that the higher dielectric constant is more of effective on gain enhancement. For example, in a study by Li et al., 2017, several different superstrate dielectric lens layers with ϵ =10.2 were used to increase the gain of a patch antenna with ϵ= 3.5 substrate. Moreover, the lens sizes used for gain enhancement are almost four times the size of the patch of the reference antenna (Li *et al.,* 2012; Adel *et al*., 2016).

In this study, the same dielectric materials are used for the substrate and superstrate, and thus the beneficial effect of the MM lens layers to the gain enhancement is more clearly shown. In addition, the total size of the MM lens layer is almost the same as the patch size of the reference antenna. The purpose and conclusion of this study are to achieve directivity enhancement with a metalayer in the dimensions between the patch size and the ground plate size of the reference antenna, and utilizing the same dielectric substrate with MM and reference antenna, unlike the literature studies. Furthermore, the novelty of this study lies in the design and behavior of the hybrid structure composed of less number of metamaterial unit cells compared to the previous works (Brito *et al,* 2012; Li *et al*, 2012; Adel *et al*., 2016; Arora *et al*., 2018; Rao *et al.,* 2016).

SIMULATION, MODELLING, AND MEASUREMENT OF THE PATCH ANTENNA

The fundamental resonance behaviors of MM resonator structures are modeled as an LC resonance circuit (Shadrivov *et al.*, 2015) and the resonance frequencies are very sensitive to the change in the capacitive and inductive effects in the geometric shape of these structures. Since the inductive and capacitive effects also vary according to the size and shape of the structure, precise measurements are required in the process of modeling and scaling. These experiments need to be done with a simulation and modeling program before production since it will be very difficult and costly to perform these analyses by physical prototyping of the structure, as well as investigating the frequency band in which the media parameters (ε, μ) have negative values. Modeling, scaling, and simulations are performed with the Computer Simulation Technology Microwave Studio (CST MWS).

The transmission bands of the patch antennas vary depending on the size of the patch and the properties of the dielectric substrate that is used (Balanis, 1997). Several experiments are needed to determine the resonance frequency range. A copper-coated Rogers RO4350B is used as a dielectric substrate. The relative dielectric constant (ε_r) is 3.48, the dielectric loss tangent is 0.0037, and the thickness is 0.762 mm. For impedance matching, two adjacent parallel slits are extended until the desired resonance input impedance value (50 Ω) is achieved (Balanis, 1997). The dimensions of the patch antenna according to the parameters in Figure 2 are given in Table 1. The reference MPA, as shown in Figure 2, is fabricated by LPKF ProtoMat S63 in-house prototyping machine.
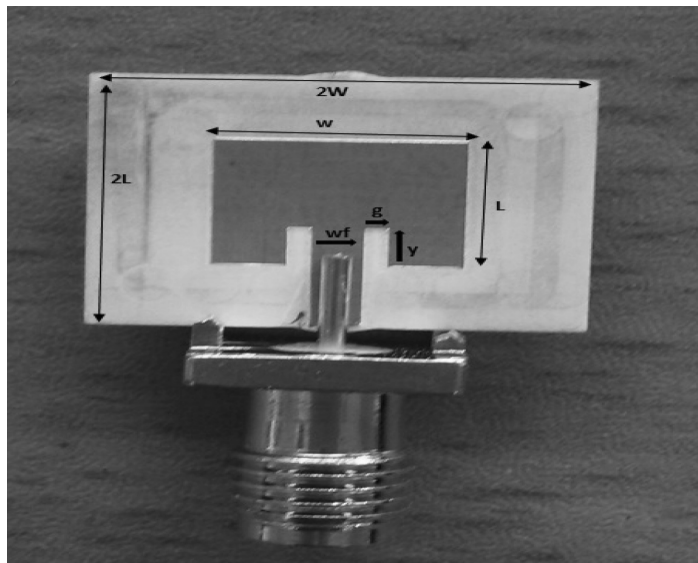
Figure 2. Top view of the reference MPA.

Table 1. Dimensions of MPA.

Parameter	Dimension (mm)
W	8.35
L	6.38
g	0.85
y	1.91
wf	1.7

S_{11} curve of the designed MPA is given in Figure 3. According to the measurement and simulation results, the transmission band is around 12 GHz and in this frequency input match is 25.2 dB / 19.3 dB (simulation/ measurement).
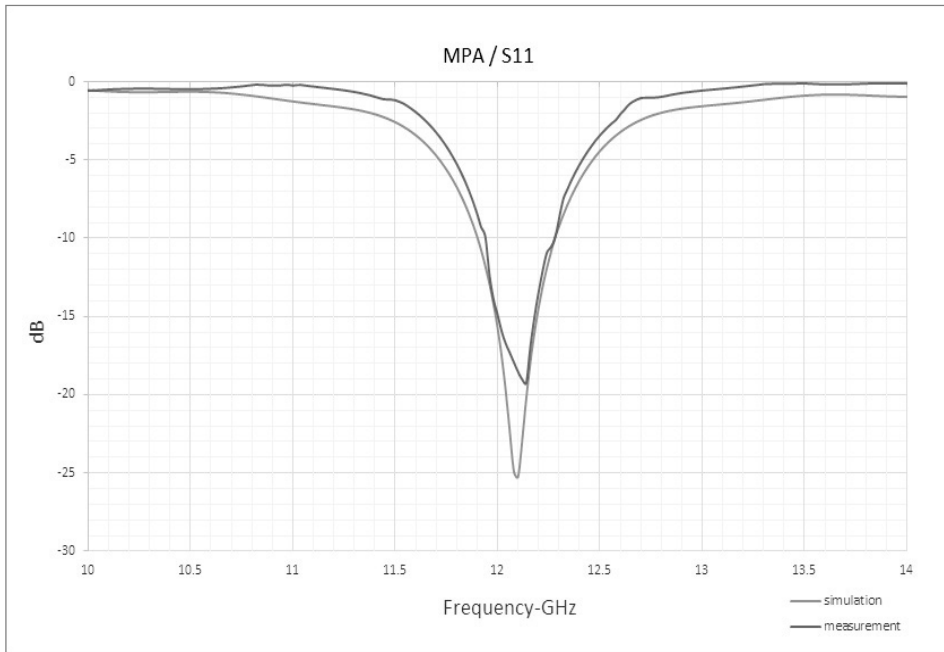

Figure 3. S_{11} curve of the MPA.

In order to view the increase in the directivity with OSM lens, the far field directivity pattern of the MPA without OSM is initially drawn for 12 GHz. The peak directivity is found as 4.66 dBi / 4.32 dBi (simulation/ measurement) as shown in Figure 4.
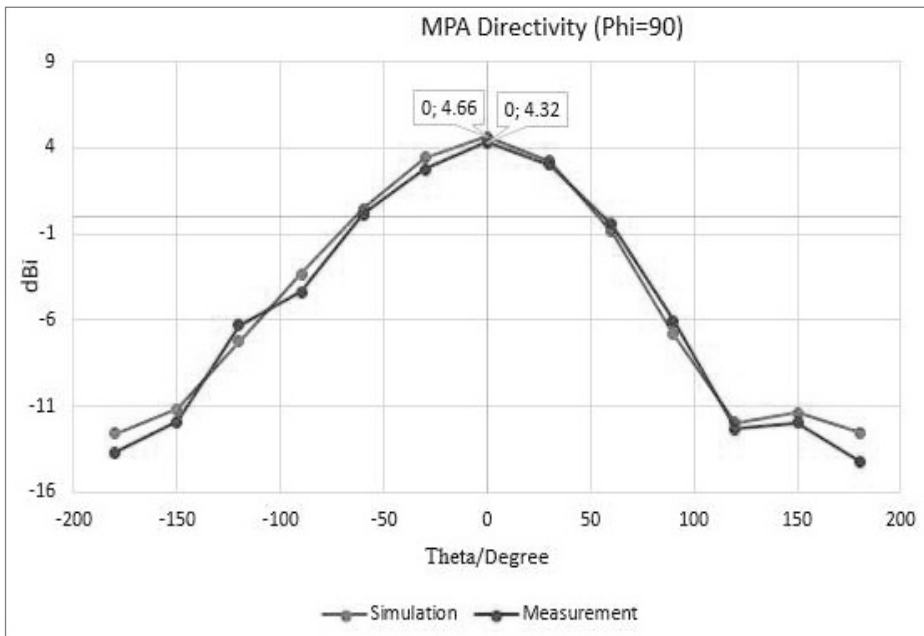

Figure 4. Directivity pattern of the MPA at 12 GHz.

OSM UNIT CELL AND EXTRACTION OF MEDIA PARAMETERS

OSM is a new type of MM structure that is designed for C, X, or THz bands in previous studies (Agarwal *et al.,* 2016; Gui *et al*., 2017; Braaten *et al.,* 2010). In this study, we designed an OSM for the Ku band with 12 GHz operating frequency and investigated the media parameters. In OSM unit cell, the same substrate with predefined characteristics and dimensions for MPA is used. There is an omega shape on the front side of the substrate and on the backside, there is symmetry of this structure with respect to the X-axis. To adjust the resonance frequency around 12 GHz, a "k" multiplier is defined on the parameter list on CST MWS. The shape and equivalent circuit of the designed OSM are shown in Figure 5 and the dimensions are given in Table 2.

a)

b)
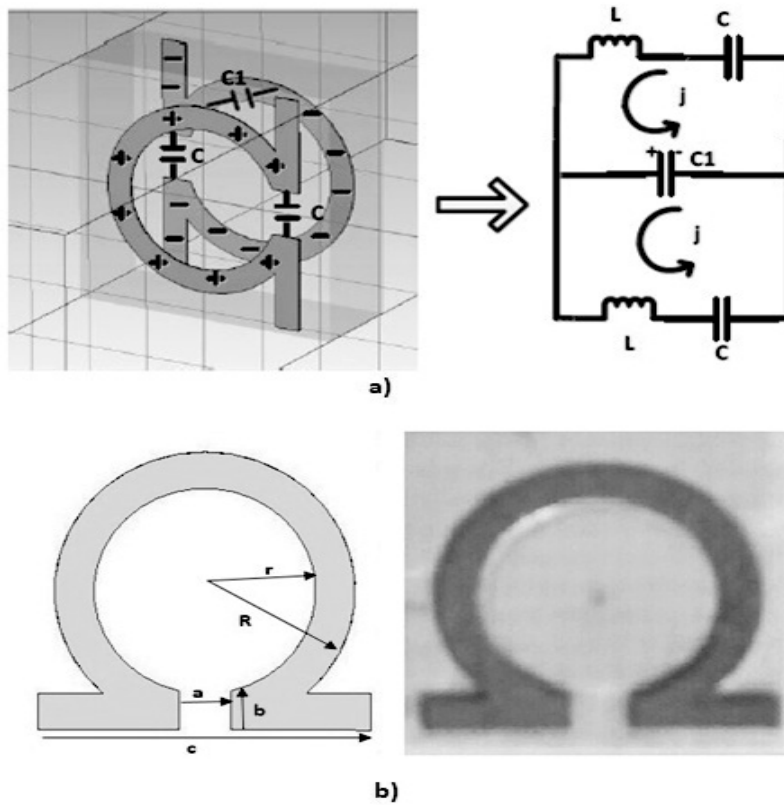
Figure 5. OSM unit cell: a) equivalent circuit; b) shape and prototype.

Table 2. Dimensions of OSM unit cell.

parameter	Dimension (mm)
a	0.88
b	0.4
c	5.6
R	2.53
r	1.87

S_{11} curve of the OSM unit cell is seen in Figure 6. The transmission band is between 11.34 GHz and 13.02 GHz. The bandwidth is 1.68 GHz and the input match (S_{11}) at 12 GHz is approximately -40 dB.
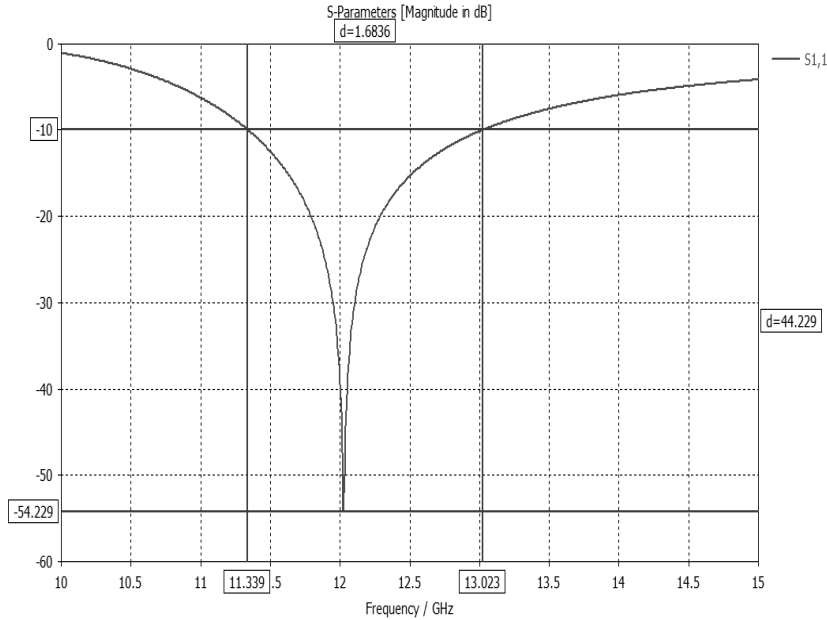

Figure 6. S_{11} curve of the OSM unit cell.

RETRIEVAL OF MEDIA PARAMETERS

There are several different methods such as Nicholson-Ross-Weir (NRW) (Soleimani *et al.,* 2012) and robust method (Chen *et al.,* 2004) to obtain the media parameters (ε and μ) from the S parameters. In this study, we chose the "robust method" and realized this method briefly as follows: initially S parameters of the OSM unit cell are obtained from CST MWS and saved to an excel file. S_{11} and S_{21} values are taken for the relevant frequency values. By defining a matrix, the primary column is defined as the frequency, the secondary column as S_{11}-real, the third column as S_{11}-imaginary, the fourth column as S_{21}-real, and the fifth column as S_{21}-imaginary. S values are placed in the columns of the excel file in the same order and the ϵ and μ curves are plotted by utilizing the equations that are given below in this method by MATLAB.

$$Z = \pm\sqrt{\frac{(1 + S_{11})^2 - S_{21}^2}{(1 - S_{11})^2 - S_{21}^2}} \tag{1}$$

$$e^{jnk_0d} = \frac{S_{21}}{1 - S_{11}\dfrac{z-1}{z+1}} \tag{2}$$

$$n = \frac{1}{k_0 d}\left\{\left[\ln\left(e^{jnk_0d}\right)\right]'' - j\left[\ln\left(e^{jnk_0d}\right)\right]'\right\} \tag{3}$$

$$\epsilon_{eff} = \frac{n}{z} \tag{4}$$

$$\mu_{eff} = n.z \tag{5}$$

In this study, we investigated whether the OSM is MM or not, so we have considered only the transmitted part of the electromagnetic waves. Thus, the imaginary parts that represent the "loss energy" are ignored (Çakır *et al.,* 2017). The ϵ and μ curves of OSM unit cell are shown in Figure 7. Notice that ϵ = -1.79 and μ= -1.9 at 12 GHz are both simultaneously negative at the same frequency.
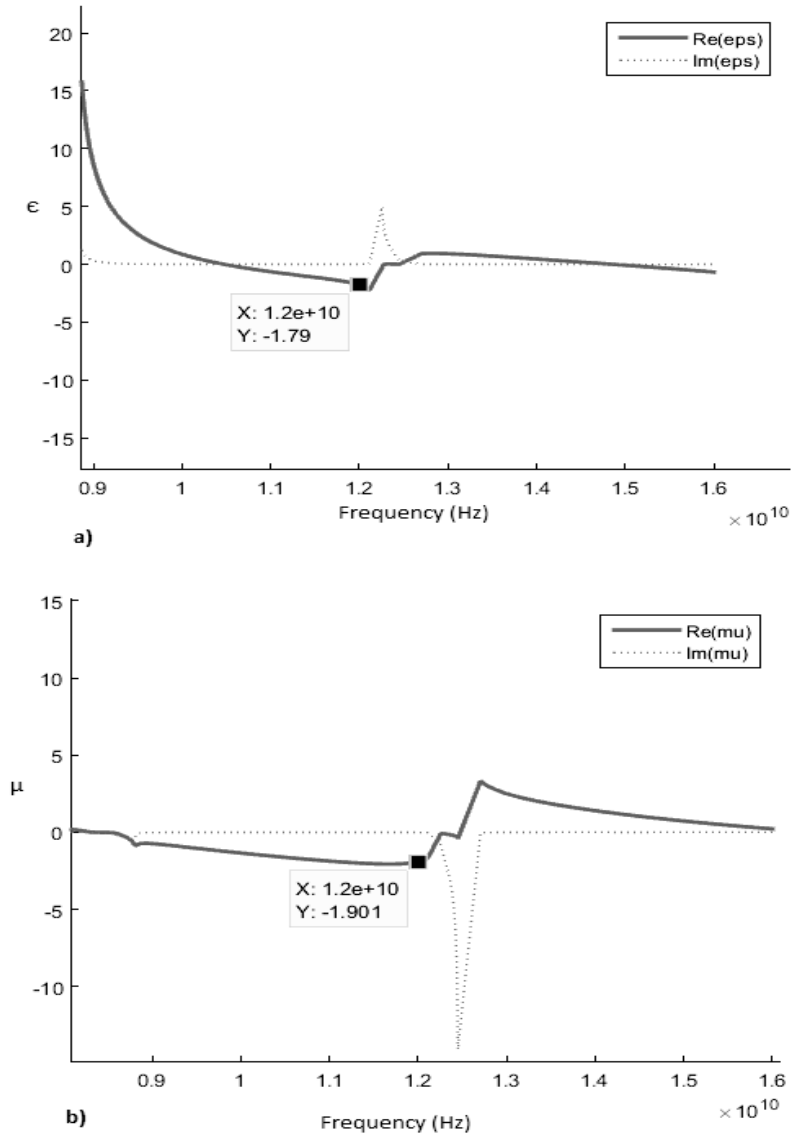
Figure 7. a) ϵ and **b)** μ curves of the OSM unit cell.

OSM AS A PERIODIC FLAT LENS

According to the Floquet theory, a single unit cell of the full periodic structure is taken into account for the analysis of periodically repeating structures such as frequency selective surfaces (FSS) and MMs (Chou *et al.*, 2015). After the unit cell studies, a MM periodic structure is formed and changes in antenna directivity are observed. Initially several parametric studies were carried out in different quantities for a periodic structure to obtain optimal input match and optimal radiation parameters and a 2 × 2 array at 12 mm × 12 mm dimensions were noted optimal, so the prototype of OSM lens was printed according to this period. Also, to define the optimum distance of this lens to the reference MPA,

several experiments are carried out and $\lambda_0 / 2 = 12.5$ mm is preferred. The top view and bottom view of the fabricated OSM lens structures are as shown in Figure 8.
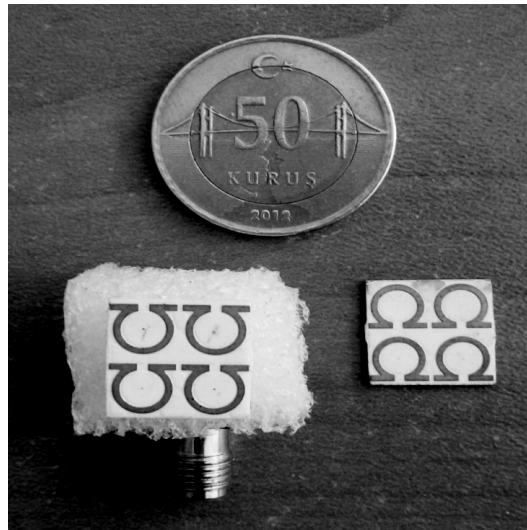

Figure 8. OSM lens prototype.

SIMULATION AND MEASUREMENT RESULTS OF MPA WITH OSM

For simulation, the boundary conditions are set to "open (add space)" in all directions on CST MWS. This option is recommended for antenna problems and adds some extra space for far field calculation. It accepts "free space" behind their boundary plane that means the electromagnetic fields are absorbed at these boundaries with virtually no reflections (www.cst.com). Figure 9 shows simulation setup.
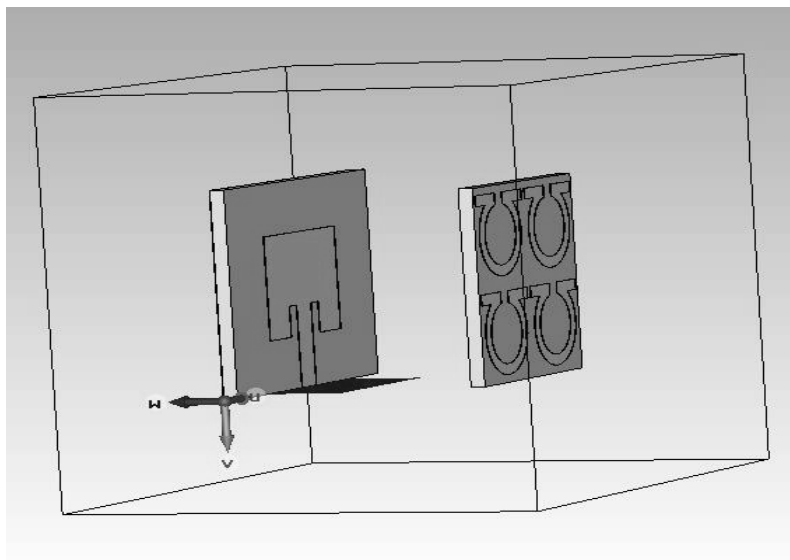

Figure 9. Simulation setup.

The radiation pattern of MPA with OSM lens is measured by using the free space measurement setup at RF and Microwave Laboratory as seen in Figure 10. A-INFO LB-8180- NF horn antennas and a vector network analyzer (Anritsu MS4644A) are used.
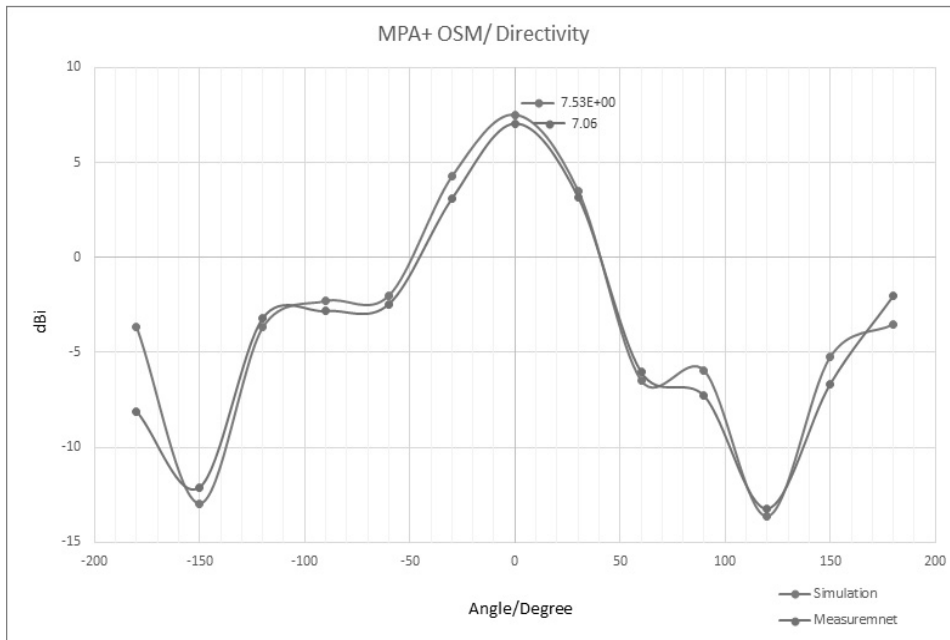
Figure 10. Measurement setup.

Figure 11 shows S_{11} curve and Figure 12 shows simulated and measured far field directivity pattern of the MPA with single layer OSM and enhancement on the directivity are given in Table 3.
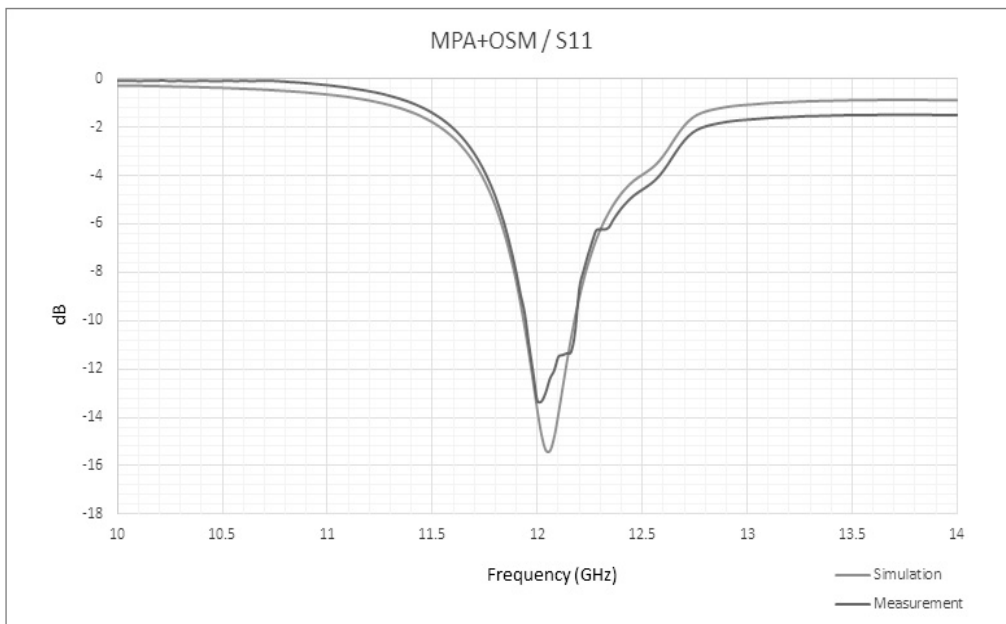
Figure 11. S_{11} curve of the MPA with OSM.

Figure 12. Far field directivity pattern of the MPA with OSM.

Table 3. Changes on directivity of the MPA with single layer OSM.

Name		Directivity (dBi)
MPA	Sim.	4.66
	Mea.	4.32
MPA+OSM	Sim.	7.53
	Mea.	7.06
CHANGE	Sim.	+2.87
	Mea.	+2.74

Omega structures are strong magnetic resonators due to their round ring as an inductor and a slot causing capacitive effect, and they give both electrical and magnetic responses at certain bandwidths of the induced electromagnetic waves. If they can be set as an inverse refraction metamaterial at certain frequencies, it is possible to use these omega structures as a lens layer for gain enhancement up to about 2 times by one layer, as shown in table 3.

MPA WITH TWO OSM LENS LAYERS

In this section, we investigate the effect of using double OSM lens layer with the same optimal distance to the reference antenna (d1=λ0 / 2 = 12.5 mm) and with the same optimal unit cell distribution on the substrate (2 × 2). The measurement and simulation scheme is shown in Figure 13.

Figure 13. Side view of the antenna system with two OSM lens layers.

The second OSM lens layer is placed parallel to the first layer. The distance between the two OSM metalayers (d2) is taken at three different values as follows; $\lambda_0 / 2 = 12.5$ mm, $\lambda_0 / 4 =\sim 6$ mm, and $\lambda_0/8 =\sim 3$ mm, and the changes in the directivity in these three different values are observed. Measurement and simulation results were obtained for these three cases. In Table 4, the peak values of the directivity are given comparatively.

Table 4. Changes on directivity of the MPA with two OSM layer.

Distance between first OSM layer and MPA	Distance between two OSM layers	MYA+2 OSM lens layer Directivity		CHANGE	
d1	d2	Simulation	Measurement	Simulation	Measurement
$\lambda_0/2=12.5$ mm	$\lambda_0/2=12.5$ mm	8.04 dBi	7.64 dBi	+3.38	+3.32
$\lambda_0/2=12.5$ mm	$\lambda_0/4=\sim6$ mm	8.28 dBi	7.92 dBi	+3.62	+3.6
$\lambda_0/2=12.5$ mm	$\lambda_0/8=\sim3$ mm	8.82 dBi	8.40 dBi	+4.16	+4.08

The optimum distance between the reference antenna and the first layer was determined as d1 $=\lambda_0/2= 12.5$ mm in the previous section and in this section, the optimal distance of the second layer to the first layer is d2= $\lambda_0 / 8 =\sim 3$ mm as shown in Table 4 and with a single layer, the increase in the directivity was 2.74 dB but when double OSM layer is used, this increase is 4.08 dB according to the measurement results. Thus, we can say that the directivity of the MPA can be further increased by using three or more lens layers, but in this case the size of the antenna system will be increased, and this is undesirable.

CONCLUSION AND DISCUSSIONS

In this study, omega shaped metamaterial lens layer is used to increase the directivity of the MPA as a flat lens. According to measurement results, a 2.74 dB increase was achieved by utilizing single layer and when the number of layers was increased by one, the increase in directivity rose to 4.08 dB. In the literature, the size of metalayers used to achieve directivity enhancement is extensive than the patch dimensions of the reference antenna, but in this study, we achieve this increase with a size between the patch and the ground plate dimensions as well as using the same dielectric substrate with reference antenna. However, this work is efficient so that it benefits over same antennas found in literature at Ku band. The measurement results are slightly different from the simulation results. It is estimated that this difference is due to media losses and fabrication defects.

REFERENCES

Adel, B.A. & Ahmed A., 2016. Metamaterial enhances microstrip antenna gain. Microwaves RF **7**: 46-50.

Agarwal, M., Behera, A.K. & Meshram, M.K. 2016. Dual resonating C-band with enhanced bandwidth and broad X-band metamaterial absorber. Applied Physics A **122**(3): 166-178.

Arora, C., Pattnaik, S.S. & Baral, R.N. 2018. Metamaterial inspired DNG superstrate for performance improvement of microstrip patch antenna array. International Journal of Microwave and Wireless Technologies, **10**(3): 318-327.

Balanis, C.A.1997. Antenna Theory: Analysis and Design. John Wiley and Sons, New York.

Braaten, B.D., Scheeler, R.P., Reich, M., Nelson, R.M., BauerReich, C., Glower, J. & Owen, G.J. 2010. Compact metamaterial-based UHF RFID antennas: Deformed omega and split-ring resonator structures. Aces Journal **25**: 530–542

Brito, D.B., d'Assuncao, A.G., Manicoba, R.H.C. & Begaud, X. 2012. Metamaterial inspired Fabry Perot antenna with cascade frequency selective surfaces. Microw Opt Technol Lett, **54**: 242-246.

Çakır, M., Koçkal, N.U., Özen, Ş., Kocakuşak, A. & Helhel, S. 2017. Investigation of electromagnetic shielding and absorbing capabilities of cementitious composites with waste metallic chips. J Microwave Power EE 51, 31-42.

Cao, W., Ma, W., Peng, W. & Chen, Z.N. 2019. Bandwidth-Enhanced Electrically Large Microstrip Antenna Loaded with SRR Structures. IEEE Antennas and Wireless Propagation Letters. doi: 10.1109/LAWP.2019.2896384.

Chen, X., Grzegorcezyk, T.M., Wu, B.I., Pacheco, J. & Kong, J.A. 2004. Robust method to retrieve the constitutive effective parameters of metamaterials. Phys Rev E **70**: 1-7.

Chou, H.T. & Tuan, S.C. 2015. Floquet modes- based asymptotic analysis of scattering from FSS- type reflect array/transmit array for near- zone- focused radiations. Radio Science 50(12), 1286-1300.

Dhouibi, A., Nawaz Burokur, S., de Lustrac, A. & Priou, A. 2013. Metamaterial-based half Maxwell fish-eye lens for broadband directive emissions. Applied Physics Letters, **102**(2): 024102.

Gui, Y., Chen, H., Yang B., Liu, J., Chen, X., Wang, X. & Yang, C. 2017. Flexible omega-ring metamaterial sensor with ultrahigh sensitivity in the terahertz region. Optical Materials Express, **7**(11): 4123-4130.

Li, D., Szabó, Z., Qing, X., Li, E.P. & Chen, Z.N. 2012. A high gain antenna with an optimized metamaterial inspired superstrate. IEEE transactions on antennas and propagation, **60**(12): 6018-6023.

Li, Q.L., Cheung, S.W., Wu, D. & Yuk, T.I. 2017. Microwave Lens Using Periodic Dielectric Sheets for Antenna-Gain Enhancement. IEEE Transactions on Antennas and Propagation, **65**(4): 2068-2073.

Ma, B., Yang, X.M., Li, T.Q., Du, X.F., Yong, M.Y., Chen, H.Y. & Zhou, L. 2016. Gain enhancement of transmitting antenna incorporated with double-cross-shaped electromagnetic metamaterial for wireless power transmission. Optik-International Journal for Light and Electron Optics, **127**(16): 6754-6762.

Mousavi, R.Z., Rezaei, P. & Zaman, M.E. 2013. Improving the bandwidth of high gain Fabry-Perot antenna using EBG substrate. Int J Nat Eng Sci, **7**(2): 78-81.

Pendry, J.B. 2000. Negative refraction makes a perfect lens. Phys Rev Lett **85**: 3966–3969.

Rao, N. & Vishwakarma, D. 2016. Gain enhancement of microstrip patch antenna using Sierpinski fractal-shaped EBG. International Journal of Microwave and Wireless Technologies, **8**(6): 915-919.

Shadrivov, I.V., Lapine, M. & Kivshar, Y.S. 2015. Nonlinear, tunable and active metamaterials. Springer, Cham, Switzerland.

Soleimani, H., Abbas, Z., Yahya, N., Soleimani, H. & Ghotbi, M.Y. 2012. Determination of complex permittivity and permeability of lanthanum iron garnet filled PVDF-polymer composite using rectangular waveguide and Nicholson–Ross–Weir (NRW) method at X-band frequencies. Measurement **45**(6): 1621-1625.

Su, Y. & Chen, Z.N. 2018. A flat dual-polarized transformation-optics beamscanning Luneburg lens antenna using PCB-stacked gradient index metamaterials. IEEE Transactions on Antennas and Propagation, **66**(10): 5088-5097.

Vesalago, V.G. 1968. The electrodynamics of substances with simultaneously negative values of ϵ and μ. Sov Phys Uspekhi **10**: 509–514.

Werner, D.H. & Kwon, D.H. 2015. Transformation electromagnetics and metamaterials. Springer, London.

Xu, H.X., Wang, G.M., Tao, Z. & Cai, T. 2014. An octave-bandwidth half Maxwell fish-eye lens antenna using three-dimensional gradient-index fractal metamaterials. IEEE Transactions on Antennas and Propagation, **62**(9): 4823-4828.

تحسين خاصية التّوجيه في الهوائي الشريطيّ الدّقيق بواسطة مادة خارقة ذات انكسار سالب.

*بلال توتونجو، *حميد توربي و**س. طه ايمجي

*قسم الالكترونيات وهندسة المواصلات، كلية الهندسة الكهربائية والالكترونية، جامعة يلدز التقنية، إسطنبول، 34220 تركيا

**قسم الهندسة الكهربائية والالكترونية، كلية الهندسة والعلوم الطبيعية، جامعة سراييفوالدولية،

سراييفو، 71000 البوسنة والهرسك

الخلاصة

نظراً لخاصيّة الانكسار العكسي، فإنّ الموادّ الخارقة بإمكانها تركيز الموجة الواردة ولهذا يمكن استخدامها كعدسات في الهوائيات ذات التّوجيه العالي. من أجل هذا الغرض، وفي هذه الدّراسة، بدايةً تمّ تصميم وحدة شريحة خارقة لإظهار ميزة المادّة الخارقة عند تردّد 12 جيغاهرتز ومن ثَمّ تحويلها إلى طبقة دوريّة. الهوائي المرجعيّ وطبقات المادّة الخارقة المقترحة تمّت محاكاتها وتصنيعها. لوحظ أنّ خاصية توجيه الهوائيّ المرجعيّ ارتفعت بمقدار 2.74 ديسيبل مع طبقة واحدة من المادّة الخارقة المقترحة وفقاً لنتائج القياس. في الأخير، تمّ استخدام طبقة ذات عدسة مزوجة ولوحظت زيادة قدرها 4.08 ديسيبل. في المراجع العلميّة، تكون أبعاد الطبقات المستعملة لتحقيق أفضل توجيه، أكبر من أبعاد الهوائيّ الشريطيّ الدقيق. لكن في هذه الدّراسة، تمّ تحقيق تحسّن كبير باستخدام طبقات من مادة خارقة أبعادها مساوية تقريبا لأبعاد الهوائيّ. غير أنّ نظام الهوائي المقترح في الدراسة أكثر فعالية من هوائي Ku band المستعمل في المراجع بفضل خاصية توجيهه العالية مقارنة بالأنظمة الأخرى.

الكلمات المفتاحية:

مادة خارقة – هوائي شريطي دقيق – LHM – توجيه الهوائي